RHEOLOGICAL PROPERTIES AND MELT-SPUN FIBER CHARACTERISTICS OF POLYMERIC NANOCOMPOSITES

Seung Hwan Lee, Jae Ryoun Youn
School of Materials Science and Engineering, Seoul National University

Keywords: *nanocomposites, compatibilizer, layered silicate, rheology, fiber spinning*

Abstract

Polypropylene/layered silicate nanocomposite fibers are prepared by melt spinning in the presence or absence compatibilizer in order to examine the influences of dispersion state and interaction force on rheological properties of the nanocomposite. The results of compatibilized nanocomposite fiber performed in the same spinning conditions were compared to polypropylene and uncompatibilized nanocomposite fiber. The tensile properties of as-spun and drawn fibers were measured and related to the melt spinning conditions, organoclay and compatibilizer contents, and the results of structural characterization. The nanocomposite fibers with organoclay and compatibilizer did not show improved tensile strength and elongation at break. The counter effect of PP-g-MAH compatibilizer played key role in internal structure and tensile property of nanocomposite fibers. The positive effect makes more effective exfoliated structure of organoclay in polymer matrix and has higher crystallinity. On the contrary, negative effect is that nanocomposite fiber has lower molecular weight than pure polypropylene fiber because compatibilizer has low molecular weight. The presence of PP-g-MAH compatibilizer gives more effective exfoliation of organoclay in nanocomposite fiber during drawing process. The tensile properties of nanocomposite fibers can be understood in terms of drawing which produces additional exfoliation of organoclay during the fiber spinning and drawing.

1 Introduction

Reinforcing fillers are inert and solid materials which are dispersed in the polymer matrix, without significantly affecting the molecular structure of the polymer matrix. Recently, there has been interest in the development of polymer composites to improve the properties of polymer matrix by reinforcement with fillers, such as carbon nanotubes or layered silicates clay. Generally nanocomposites are defined by the filler size of the dispersed phase, with at least one dimension less than 100 nm. If the dispersion at the nanoscale level is homogeneous, it leads to physical properties of the material that are difficult to attain from individual components. These nanocomposites have potential for applications as functional materials [1-2].

While polymer/layered silicate nanocomposites were first reported in 1960s, researches were not studied further until 1990s because suitable applications were not invented. However, hybrid nanocomposites comprising organically modified layered silicates dispersed in selected polymer matrices have attracted attention with the advantage that they are efficient at concentrations of 5 wt% or less [3-4]. Several kinds of fillers can be used to enhance the mechanical properties of polymer matrix, such as modified montmorillonite and titanium dioxide. Of these all, the ion-exchanged montmorillonite is the most common one because of its superior geometry characteristics and low price. To improve dispersion within an organic polymer, however, these sodium cations in montmorillonite must be replaced by cations that are sufficiently organophilic. This usually requires the use of an ammonium or phosphonium salt that contains at least one alkyl chain which is 14 or 16 carbons in length. Also, the other substituents on the onium salt may be freely chosen in order to enhance some particular property of the nanocomposite [5].

Especially PP/layered silicate nanocomposites are attractive systems that can lead to new materials

for engineering applications and widen the versatility of polypropylene based materials. However, there has been a limitation on the polymer used for layered silicate reinforced nanocomposites. The homogeneous and fully exfoliated dispersion of the silicate layers could be achieved in case that such as polymers with polar functional groups. This is mostly due to the fact that the silicate layers of the organoclay have polar hydroxy groups and are compatible with polymers containing the functional groups [6-7]. On the other hands, poor adhesion between the filler surface and the polymer matrix prevents necessary wet-out by molten polymer to help break up aggregates of particles, resulting in poor dispersion, insufficient reinforcement, and poor mechanical properties. To overcome these problems, first method is to make the surface more hydrophilic by treating the filler with a surface treatment. Another approach is to modify the chemistry of the PP matrix by attaching polar group, such as maleic anhydride based polymer.

Fiber melt spinning involves preparation of a spinning fluid by melting polymeric material or direct polymerization, extrusion of the melt through spinnerets into a cooling chamber, and winding of the resulting filaments. New technologies have been developed in the past years with the goal of integrating as many production steps as possible into a single continuous process. However, most of macron scale fillers are unsuitable for fiber spinning because they can easily lead to spinline failures due to their size that approach the order of the diameter of the fibers themselves. Because of reduced thickness and extremely large aspect ratio, the interaction between the reinforcing filler and polymer matrix is maximized due to the increase in contact area. Consequently, the nanofiller loading could be reduced to 1-5 wt% while providing similar property enhancement as the macrocomposites at high concentrations [8-10].

Mlynarcikova et al. [11] investigated that fiber spinning characteristics of nanocomposites prepared from syndiotactic polypropylene and layered silicate organoclay with octadecylammonium chains and reported that only using with the compatibilizer high draw ratio of the nanocomposite fibers was achieved. According to their reports, most experimental results indicate that the counter effects of the low molecular weight of compatibilizer prevails over positive effect of the organoclay on tensile properties of PP/layered silicate nanocomposites. Also, Zheng et al. [12] examined the internal structure and mechanical properties of the PP/clay nanocomposites and hybrid

nanocomposite fibers using various characterization methods. The nanometer scaled organoclay layers dispersed in the PP matrix actually played the role of heterogeneous nuclei species in the process of PP crystallization and increased the nucleation speed of the nanocomposites, leading to the increase of crystallization rate of the as-spun fibers. Meanwhile, it was found that the crystallinity of nanocomposite fibers is much higher than that of pure PP fiber at the same draw ratio, whereas the orientation of hybrid fibers is much lower than that of pure PP fiber at the same draw ratio.

In this study, exfoliated polypropylene/layered silicate nanocomposites are prepared using malated polypropylene (PP-g-MAH) and investigated morphological and rheological properties. Then, fiber melt spinning is performed to evaluate effects of spinning conditions on formation of internal structure and tensile property of nanocomposite fibers. Finally, their nanocomposite characteristics are explained through the correlation among the spinning condition, organoclay and compatibilizer content, and structural parameters such as the degree of exfoliation and crystallinity in nanocomposite fibers.

2. Experimental

2.1 Materials

The nanocomposites consisted of isotactic polypropylene (iPP), which is used as a matrix, layered silicate orgarnoclay (OLS), and PP-g-MAH compatibilizer. The PP resin was obtained from Polymirae (MOPLENE HP552N). It had a melt flow rate (MFR) of 12.0 g/10min and melting point of 162℃. Na$^+$-based montmorillontie with a cation-exchange capacity value (CEC) of 125 mmol/100g and organoclay were prepared in Southern Clay Products (Cloisite®15A, USA). PP-g-MAH compatibilizer supplied from Crompton (Polybond® 3150, USA) to promote the interaction due to hydrogen bonding between PP matrix and organoclay layers. Its MFR was 50 g/10min and grafted maleic anhydride (g-MAH) content was 0.5 wt%.

2.2 Melt compounding and fiber formation

All samples were prepared via melt compounding at 210℃ and at a screw speed of 350 rpm by using a twin-screw extruder (Werner & Pfleiderer, ZSK-25 type). The compounded melt was water quenched and pelletized. Before melt

spinning, the pure polypropylene and nanocomposite pellet were dried in a vacuum oven for 4 hrs at 80℃. Melt spinning was performed on a single screw extruder (Length/Diameter=30, Polymirae, KOREA) with a spinneret containing 60 holes, each 0.5 mm in a diameter and 1.0 mm in a length. The extruder was set with four different temperature zones of 190, 210, 230℃, and 240℃ at feed, metering, melting, and spinneret sections, respectively. The as-spun filaments were collected at a take-up speed of 500-1,250 m/min and drawn (draw ratio λ = 1 - 4) at 120℃. The processing machine is presented in Fig. 1.

Fig. 1. Melt spinning machine used in this study.

2.3 Characterization

2.3.1. Morphology

Small angle X-ray scattering by Rigaku Max-3 Cg X-ray diffractometer with Cu-Kα radiation (λ=0.154184 nm) was used to determine the interlayer spacing of clays for PP/layered silicate nanocomposites. The wide-angle X-ray diffraction patterns of the polypropylene nanocomposite fibers were obtained by using X-ray diffraction (BRUKER AUX D8 Advance with GADDS, 40 kV, 40 mA, Cu-Kα) in a scanning range of 0 - 40^{o}(2θ).

2.3.2. Rheological properties

Dynamic oscillatory shear flow measurements were conducted using a rotational rheometer (AR-2000, Rheometric Scientific) with parallel plates. Frequencies of 0.01 - 200 rad/s were used at the strain amplitude of 10% in order to be within the linear viscoelastic region. The viscosity growth during uniaxial elongational flow at a constant elongation rate was measured using a Meissner-type rheometer (RME, Rheometric Scientific). The

constant elongation rates, $\dot{\varepsilon}_0$, were applied at elongation rates of 0.05, 0.1, 0.3, 0.5 and 1.0 s^{-1}. The MFR of various samples was measured by weighing the run for 10 minutes under 2.16 kg at 230℃ using a melt flow indexer (Melt Flow Rate, Göttfert).

2.3.3. Tensile properties

The fiber's linear density of fibers was determined at ambient temperature using a Zweigle L232. The tensile strength and elongation at break of the non-filled and isotactic PP nanocomposite fibers were determined at an ambient temperature using an Uster Tensorapid-4 (Zellweger Uster). Gauge length was 200 mm and deformation rate was 100 mm/min for as-spun and drawn fibers. The tensile strength and elongation at break of fibers were calculated from the stress-strain curve. The tensile strength was determined from the top of the stress-strain curve and elongation at break was determined from the distance between the start and the point of break.

3 Results and discussion

3.1. Morphology of compounded nanocomposites

Figure 2 shows the SAXS for organoclay powders, uncompatibilized, and compatibilized nanocomposites. The SAXS pattern of the original organoclay shows the peak of intensity at the diffraction angle of $2\theta = 2.65°$ and the equivalent distance between silicate layers is 34.46Å. The SAXS pattern of PP-g-MAH compatibilized nanocomposites does not show the characteristic basal peak of the organoclay. It is indicated that the strong interaction between polar group of compatibilizer and functional group of the silicate layer had formed and polypropylene chains had intercalated into the galleries of organoclay.

However, SAXS spectra patterns of the organoclay filled PP nanocomposites display a slight increase in the intensity at lower 2θ values when compared with that of the unfilled polymer matrix. As can be seen from Fig. 2, both uncompatibilized and compatibilized nanocomposite systems with organoclay shows weak (002) plane peaks at about $2\theta = 3.32°$. This is probably that thermal degradation of ion-exchanged organoclays had been occurred during melt compounding. Otherwise, it is assumed that there was insufficient shear stress to exfoliate the organoclay during melt compounding because of low molecular weight of PP matrix (MFR 12.0 g/10min) [6-7, 13].
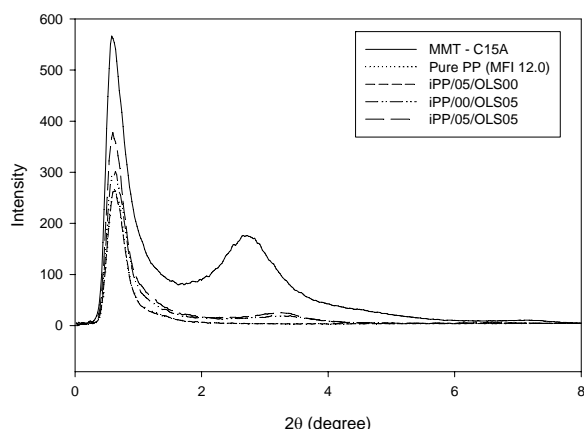
Fig. 2. SAXS patterns of organoclay powder, pure PP, uncompatibilized nanocomposite, and PP-g-MAH compatibilized nanocomposite.

X-ray scattering is useful for the measurement of the distance spacing of ordered intercalated nanocomposites with organoclay, but it may be insufficient for the measurement of disordered and exfoliated materials that give no peak. The organoclay dispersion in polypropylene matrix was crosschecked further by using the TEM and rheological results. To observe the exfoliated structure of the silicate layers, TEM images for uncompatibilized and PP-*g*-MAH compatibilized nanocomposites are shown in Figs. 3 (a) and (b). In the case of uncompatibilized composites the silicate layers were aggregated with a size of several hundreds of nanometers in the polypropylene matrix. The micrograph of the PP-g-MAH compatibilized nanocomposites shows that individual exfoliated platelets are embedded in the polymer matrix resin. Each layer of the organoclay is dispersed homogeneously in the polypropylene matrix, although a small amount of intercalated layers still exists. It is apparent that the PP-*g*-MAH compatibilizer improved the dispersity and homogeneity of layered silicates in PP matrix.

3.2. Rheological Properties

Characteristic rheological behaviors with respect to internal structure of the nanocomposites were investigated from the information on nanoscale dispersion of clay particles in the nanocomposite. Rheological behavior of various polypropylene nanocomposites was investigated in a conventional melt state rheometer in both shear and elongational modes. Firstly, Table 1 shows the melt flow rate (MFR) decreased from 11.56 to 10.55 as the loadings of compatibilizer increased from 1.0 to 7.0 wt%. This confirms that compounded PP/layered

silicate nanocomposite melts were fluid enough to melt spin with conventional spinning machine.


(a)
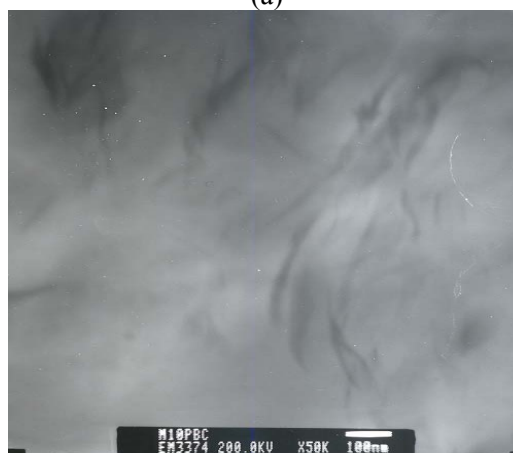
(b)

Fig. 3. TEM images of (a) uncompatibilized composites and (b) PP-g-MAH compatibilized nanocomposites.

Table 1. Influence of organoclay and compatibilizer contents for each nanocomposite system on melt flow rate (MFR).

Samples	MFR(g/10min)
iPP	12.35
iPP/PB05	13.95
iPP/00/OLS03	11.32
iPP/05/OLS03	10.64
iPP/01/OLS03	11.56
iPP/03/OLS03	11.02
iPP/07/OLS03	10.55

In Fig. 4, storage modulus and complex viscosity are compared the difference in shear flow properties between the two kinds of nanocomposite. The pure polypropylene shows classical viscoelastic behavior, a terminal flow regime where storage

modulus is proportional to ω^2. The uncompatibilized nanocomposite shows a small deviation from classical behavior at lower frequencies. There is a slight increase of storage modulus with increasing clay content and only a weak solid-like plateau behavior is observed at low frequency region [14].
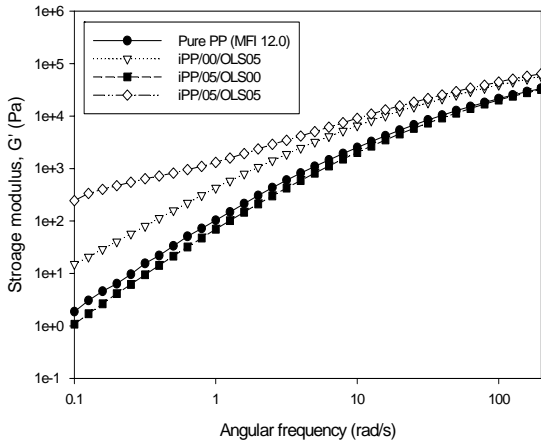

(a)
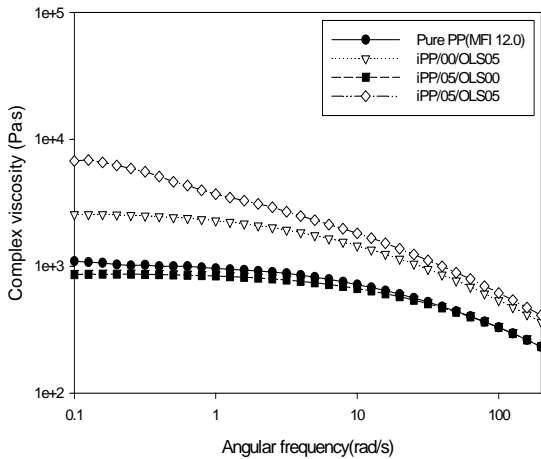
(b)

Fig. 4. Frequency dependence of (a) storage modulus and (b) complex viscosity for the pure PP, uncompatibilized, and PP-g-MAH compatibilized nanocomposites.

However, in case of PP-g-MAH compatibilized nanocomposite melts, storage modulus shows non-terminal plateau solid-like behavior and has higher value in comparison with that of pure polypropylene or uncompatibilized nanocomposites at low frequency ranges. The solid-like plateau behavior becomes distinct as the clay content is increased. As the amount of well-dispersed clay is increased, a network structure will be formed due to the close interaction between clay particles as well as

hydrodynamic interaction between clay particles and polymer chains.

Figure 5 shows the elongational viscosity observed for pure PP, uncompatibilized, and PP-*g*-MAH compatibilized nanocomposites with different elongational rates ranging from 0.01 to 1.0 s^{-1}. In pure PP matrix and uncompatibilized composites, the elongational viscosity increases linearly with time and strain hardening was not observed. In the case of PP-*g*-MAH compatibilized nanocomposite, the initial part of all the elongational viscosity growth curves showed simple monotonic growth that agreed well with the theory of linear viscoelasticity. After deformation equivalent to the *Hencky* strain ($\varepsilon = \dot{\varepsilon} \cdot t$) of about 1.0 some of the growth curves showed increase in the slope as the viscosity growth rate was accelerated, i.e., strong strain hardening was occurred. Therefore, it is expected that spinnability of compatibilized nanocomposites may be improved at higher elongational rates in the middle of fiber spinning [15].
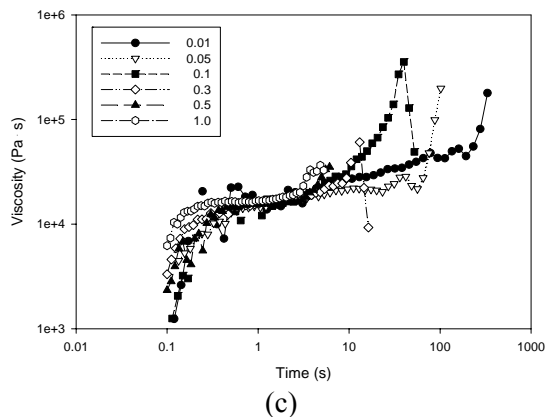

(a)

(b)

(c)
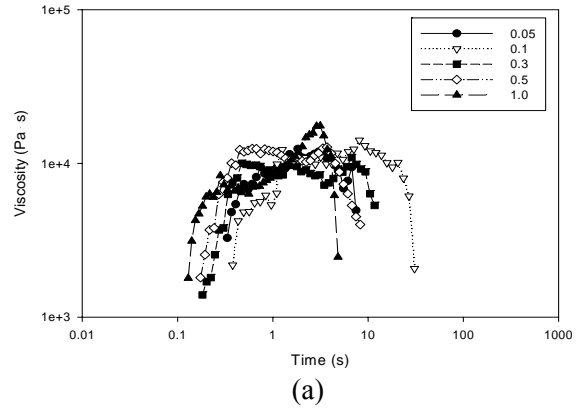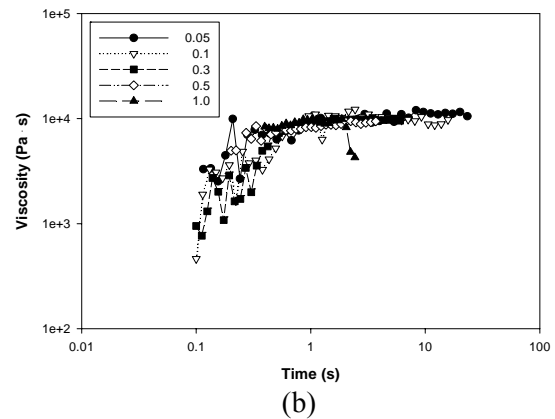
Fig. 5. Elongational viscosity growth curves of (a) pure PP, (b) uncompatibilized composites, and (c) compatibilized nanocomposite melts at different elongational strain rates (T =190℃).

3.3. Fiber properties

Polypropylene fibers are produced in a variety of types with different tenacities to apply varying market requirements. Fibers for general textile uses have tenacities in the range of 4.0 - 6.0 g/den. High tenacity fibers up to 8.0 g/den are produced for the use in industrial applications such as ropes, nets, and so on [16-17]. There are two structural parameters affect on physical properties in case of nanocomposite fiber: extent of exfoliation and degree of crystallinity. It is also important since the tensile properties depend on fiber structure and since it is sensitive to the spinning condition.

In this study, two types of PP nanocomposite fibers were prepared to investigate the correlation among mechanical properties, crystallization, and exfoliation structure. They were prepared in the presence or absence of PP-g-MAH compatibilizer having low molecular weight at the same loadings of organoclay. The tensile strength and elongation at break of pure polypropylene and its nanocomposites are plotted versus spinning speed in Fig. 6. The tensile strength of pure PP fiber increased up to 1,000 m/min and decreased thereafter. Both nanocomposite fibers, however, increased through experimental speed ranges, and extent of increase in compatibilized fiber was bigger than that of uncompatibilized nanocomposite fiber. Although elongational at break values of pure PP fiber gradually decreased at total experimental ranges, value of two types of nanocomposite fibers remained constant. It is probably that crystallinity and crystal orientation of nanocomposite fibers increased as spinning speed are increased.
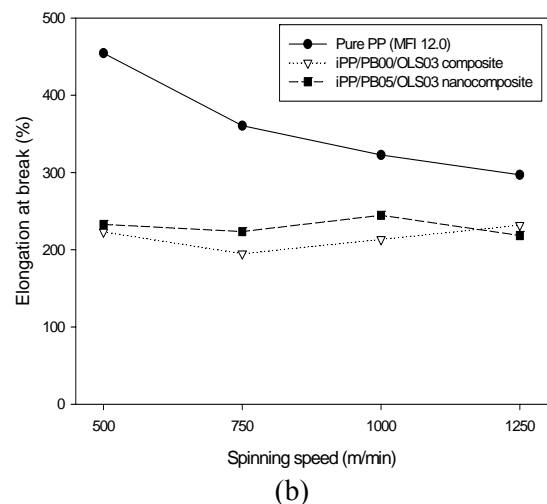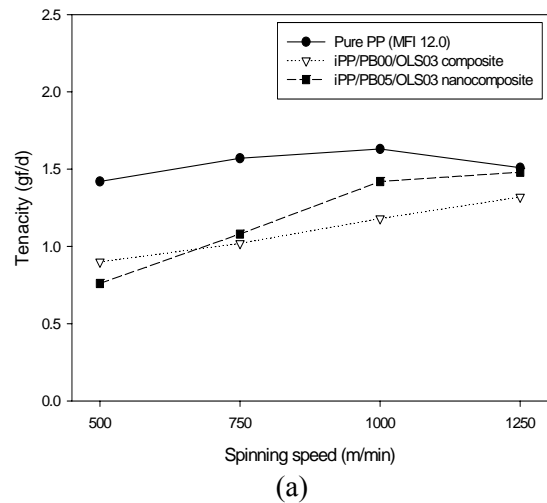

(a)

(b)

Fig. 6. Effects of spinning speed on (a) tenacity and (b) elongation at break of pure polypropylene, uncompatibilized, and PP-g-MAH compatibilized nanocomposite fibers.

The effect of organoclay and compatibilizer on crystalline morphology and exfoliation structure of pure PP and two types of nanocomposites was characterized and analyzed to connect their tensile properties. In Fig. 7, the WAXD study illustrates that the addition of organoclay and compatibilizer greatly affect the crystalline form and extent of exfoliation of as-spun nanocomposite fibers. It was found that PP fiber and nanocomposite fibers exhibit different crystalline diffraction peak intensities. However, the peak position of every crystal plane did not shift just because of addition of clay and compatibilizer, which indicated that crystallization types of nanocomposites did not change, still being α monoclinic crystal type [18].
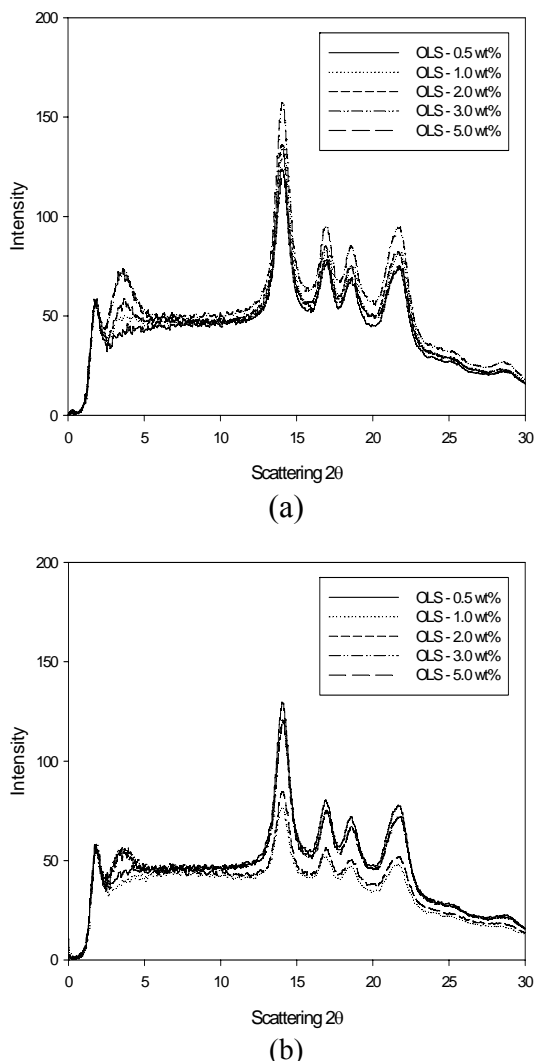
(a)

(b)

Fig. 7. Effects of organoclay loadings on the WAXD patterns of (a) uncompatibilized fibers without compatibilizer and (b) nanocomposite fibers with PP-*g*-MAH compatibilizer of 5.0 wt%.

An important observation from Fig. 7 is that relative to the intensity of the (110) peak the intensities of the other α-phase peaks, that is, (040), (130), and (041) increased with the addition of organoclay. A possible reason is that the addition of organoclay promotes the nucleation and growth of polypropylene crystals and perfects the α-phase crystallite [19-20]. The intensities of the (040) peaks were much higher than that of the (111) peak at the organoclay loading of 2.0 wt%. This fact implies that the surface of the organoclay platelets may induce a preferred orientation of the α-form crystallites. At lower organoclay contents, organoclay is well exfoliated so that the organoclay platelets can be easily oriented with fiber spinning because of their large aspect ratio. The orientation of

organoclay may lead to the orientation of the crystallites if they are initialized on the organoclay surface in a certain direction. However, when the organoclay content becomes 5.0 wt% the organoclay orientation is more difficult because of the reduced aspect ratio of organoclay, which would lead to more isotropic arrangement of crystallites [3, 21-22].

Tensile properties of nanocomposite fibers were also investigated to evaluate the reinforcing effect of the organoclay and PP-*g*-MAH compatibilizer. Figure 8 shows effects of organoclay loadings on the tensile properties of nanocomposite fiber with or without compatibilizer. At the below of 2.0 wt% of organoclay, the nanocomposite fibers with compatibilizer have a similar tensile strength compare to that of without compatibilizer. The tenacity and elongation at break values of both nanocomposite fibers remain at the level of pure PP fiber up to organoclay of 2.0 wt% and then abruptly decrease with content of organoclay. This is because the presence of PP-*g*-MAH compatibilizer gives more effective exfoliation of organoclay particles than in its absence. There are also reports that the extent of exfoliation of an organoclay in a polymer matrix should relate to the basal spacing of the organoclay. For example, Reichert *et al*. [23] indirectly showed a gradual increase in tensile properties with organoclay d-spacing, caused by the increase in the carbon number of the alkyl substituent on the onium ion, for a nanocomposite system. They found a gradual increase in tensile properties as alkyl chain length was increased from a carbon number of four to eight carbons. Increasing the alkyl length from 8 to 12 carbons resulted in a significant increase in d-spacing and a step increase in modulus. However, modulus leveled off beyond a carbon number of 12.
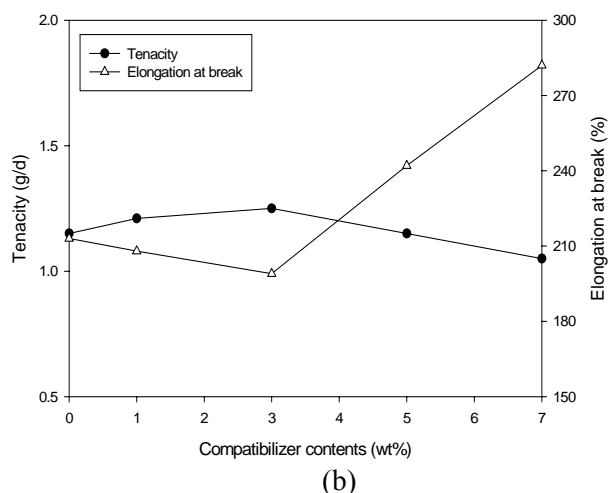

(a)

(b)
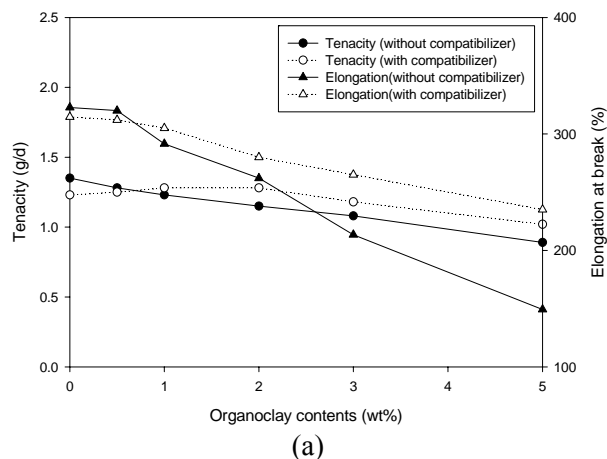
Fig.8. Effects of (a) organoclay and (b) PP-*g*-MAH compatibilizer loadings on tensile properties of uncompatibilized and compatibilized nanocomposite fibers.

In general, it is expected that larger initial layer spacing may lead to easier exfoliation since platelet-platelet attractions is reduced. It is implied that diffusion of polymer chains inside organoclay galleries is less hindered due to increased spacing and ultimately leads to improved exfoliation. For the both nanocomposite fibers with organoclay, there are small intercalated aggregates as well as well dispersed domains whose size and distribution correlate to the concentration of organoclay in the nanocomposite fibers. Low contents of organoclay result in small dispersed domains and uniform distributions, whereas high loadings results in large size and broad distributions. It is confirmed that homogeneous dispersion state of organoclay may bring better properties to the final fibers. In the PP-*g*-MAH compatibilized nanocomposite fiber, however, the extent of decrease is less than that of uncompatibilized composite fibers [8, 24-25].

The influence of compatibilizer content on tensile properties of nanocomposite fibers containing 3.0 wt% of organoclay was illustrated in Fig. 8(b). The tensile strength slightly increased up to compatibilizer of 3.0 wt% and then decreased thereafter. The elongation at break decreased up to 3.0 wt% and then increased with increasing compatibilizer. It is probably that the mechanical properties can be attributed to homogeneous distribution of organoclay and to the crystal structure of polypropylene nanocomposite fibers. From above results, it is indicated that counter effect of PP-*g*-MAH compatibilizer play key role in internal structure and tensile property of nanocomposite fibers. The positive effect makes more effective

exfoliated structure of organoclay in polymer matrix and has higher crystallinity.

On the contrary, negative effect is that nanocomposite fiber has lower molecular weight than pure polypropylene fiber because PP-*g*-MAH compatibilizer has low molecular weight. It is indicated that the positive influence prevails over negative reinforcing effect of the organoclay up to 3.0 wt% of compatibilizer. However, above 3.0 wt% of compatibilizer, negative effect predominates over the positive effect as seen from Fig. 8. The negative effect of compatibilizer on tensile strength of the nanocomposite fibers is understood as a result of the influence of its low molecular weight on the decrease of polymer chain orientation in PP/organoclay nanocomposite fibers. From above experimental results, tensile properties of nanocomposite fiber with organoclay and compatibilizer strongly depend on the crystal structure and extent of exfoliation in PP matrix. It is also expected that most effective enhancement realized at range from 1.0 to 2.0 wt% of organoclay and compatibilizer of 3.0 wt% on the tensile properties of compatibilized nanocomposite fiber.

4. Conclusion

The experimental results of compatibilized nanocomposite fiber made in the same spinning conditions were compared to polypropylene and uncompatibilized nanocomposite fiber. The tensile properties of as-spun and drawn fibers were measured and related to the melt spinning conditions, organoclay and compatibilizer contents, and the results of structural characterization. The nanocomposite filaments with organoclay and compatibilizer did not show improved tensile strength and elongation at break. The counter effect of PP-*g*-MAH compatibilizer played key role in internal structure and tensile property of nanocomposite fibers. The positive effect makes more effective exfoliated structure of organoclay in polymer matrix and has higher crystallinity. On the contrary, negative effect is that nanocomposite fiber has lower molecular weight than pure polypropylene fiber because compatibilizer has low molecular weight. It is indicated that the positive influence prevails over negative reinforcing effect of the organoclay up to 3.0 wt% of compatibilizer.

Both nanocomposite fibers have relatively low tensile strength values in comparison with pure polypropylene fiber at the same drawing ratio. They have lower tensile strength and elongation at break

caused not only by lower compatibility but also by the fact that organoclay increase the crystallization rate and decrease crystal size. It is concluded that the presence of PP-*g*-MAH compatibilizer gives more effective exfoliation of organoclay in nanocomposite fiber during drawing process. The tensile properties of nanocomposite fibers can be understood in terms of drawing which produces additional exfoliation of organoclay during the fiber spinning and drawing.

References

[1] Shenoy, A.V. "*Rheology of Filled Polymer Systems*", Kluwer Academic Publishers, 1999.

[2] Ajayan, P.M., Schadler, L.S., and Braun P.V. "*Nanocomposite Science and Technology*", Wiley-VCH, 2003.

[3] Mehta S., Mirabella F.M., Rufener K, and Bafna A. "Thermoplastics olefin/clay nanocomposites: morphology and mechanical properties", *J. Appl. Polym. Sci.*, Vol. 92, No. 2, 928-936, 2004.

[4] Solomon M.J. and Almusalla A.S. "Rheology of Polypropylene/Clay Hybrid Materials", *Macromolecules*, Vol. 34, pp 1864-1872, 2001.

[5] Xu W., Liang G., Zhai H., Tang S., Hang G., and Pan W.P. "Preparation and crystallization behavior of PP/PP-g-MAH/Org-MMT nanocomposite", *Eur. Polym. J.*, Vol. 39, No. 7, pp 1467-1474, 2003.

[6] Kim K., Kim H., and Lee J.W. "Effect of interlayer structure, matrix viscosity and composition of a functionalized polymer on the phase structure of polypropylene-montmorillonite nanocomposites", *Polym. Eng. Sci.*, Vol. 41. pp 1963-1969, 2001.

[7] Fornes T.D., Yoon P.J., Keskkula H., and Paul D.R. "Nylon 6 nanocomposites: the effect of matrix molecular weight", *Polymer*, Vol. 42, No. 24, pp 9929-9940, 2001.

[8] Cho W. and Paul D.R. "Nylon 6 nanocomposites by melt compounding", *Polymer*, Vol. 42, No. 3, pp 1083-1094, 2001.

[9] Fornes T.D., Yoon P.J., Hunter D.L., Keskkula H., and Paul D.R. "Effect of organoclay structure on nylon 6 nanocomposite morphology and properties", *Polymer*, Vol. 43, No. 22, pp 5915-5933, 2002.

[10] Svoboda P., Zeng C., Wang H., James Lee L., Tomasko D.L. "Morphology and mechanical properties of polypropylene/organoclay nanocomposites", *J. Appl. Polym. Sci.*, Vol. 85, No. 7, pp 1562-1570, 2002.

[11] Mlynarcikova Z., Kaempfer D., Thomann R., Mulhaupt R., Borsig E., and Marcincin A. "Syndiotactic PP/organoclay nanocomposite fibers: influence of the nano-filler and the compatibilizer on the fiber properties", *Polym. Adv. Technol.*, Vol. 16, pp 362-369, 2005.

[12] Zheng W., Lu X., Toh C.L., Zheng T.H., and He C. "Effect of clay on polymorphism of polypropylene in polypropylene/clay nanocomposites", *J. Polym. Sci.,Pol. Phys.*, Vol. 42, No. 10, pp 1810-1816, 2004.

[13] Seo Y., Kim J., Kim K.U., and Kim Y.C., "Study of the crystallization behaviors of polypropylene and maleic anhydride grafted polypropylene", *Polymer*, Vol. 41, No.7, pp 2639-2646, 2000.

[14] Larson R.L., "*The Structure and Rheology of Complex Fluids*", Oxford University Press, New York, 1999.

[15] Gahleitner M. "Melt rheology of polyolefins", *Prog. Polym. Sci.*, Vol. 26, No. 6, pp 895-944, 2001.

[16] Gupta V.B., Mondal S.A., and Bhuvanesh Y.C. "Spinning speed-throughput rate relationships for polyester, nylon, and polypropylene", *J. Appl. Polym. Sci.*, Vol. 65, No. 9, 1773-1788, 1997.

[17] Joshi M and Viswanathan V. "High-performance filaments from compatibilized polypropylene/clay nanocomposites", *J. Appl. Polym. Sci.*, Vol. 102, No. 3, pp 2164-2174, 2006.

[18] Wunderlich B. and Grebowicz J. "Thermotropic mesophases and mesophase transitions of linear, flexible macromolecules", *Adv. Polym. Sci.*, Vol. 60/61, pp 1-36, 1984.

[19] Nurul Huda M., Dragan H., Bauer S., Muschik H., and Skalicky P. "A study of the crystallinity index of polypropylene fibers", *Colloid Polym. Sci.*, Vol. 263, No. 9, pp 730-737, 1985.

[20] Sculdla J., Raab M., Eichborn K.J., and Strachota A. "Formation and transformation of hierarchical structure of β nucleated polypropylene characterized by X-ray diffraction, differential scanning calorimetry and scanning electron microscopy", *Polymer*, Vol. 44, No. 16, pp 4655-4664, 2003.

[21] Pavlikova S., Thomann R. Reichert P. Mulhaupt R. Marcincin A. and Borsig E., Fiber Spinning from Poly(propylene)-Organoclay Nanocomposite, *J. Appl Polym Sci*, Vol. 89, pp. 604-611, 2003.

[22] Zhang X. Yang M. Zhao Y. Zhang S. Dong X. Liu X. Wang D. and Xu D., Polypropylene/Montmorillonite Composites and Their Application in Hybrid Fiber Preparation by Melt-Spinning, *J. Appl Polym Sci*, Vol. 92, pp. 552-558, 2004.

[23] Reichert P., Nitz H., Klinke S., Brandsch R., Thomann R., and Mulhaupt R. "Polypropylene/ organoclay nanocomposite formation: Influence of compatibilizer functionality and organoclay modification", *Macromol. Mater. Eng.*, Vol. 275, No. 1, pp 8-17, 2000.

[24] Broda J. "WAXS investigations of mass-coloured polypropylene fibers", *Fibres Text. East. Eur.*, Vol. 11, No. 5, pp 115-119, 2003.

[25] Hasegawa N. and Usuki A. "Silicate layer exfoliation in polyolefin/clay nanocomposite based on maleic anhydride modified polyolefins and organophilic clay", *J. Appl. Polym. Sci.*, Vol. 93, No. 1, pp 464-470, 2004.